

Precision measurement of the branching fractions of  
 $J/\psi \rightarrow \pi^+\pi^-\pi^0$  and  $\psi' \rightarrow \pi^+\pi^-\pi^0$

M. Ablikim<sup>1</sup>, M. N. Achasov<sup>5</sup>, D. Alberto<sup>41</sup>, D.J. Ambrose<sup>38</sup>, F. F. An<sup>1</sup>, Q. An<sup>39</sup>,  
 Z. H. An<sup>1</sup>, J. Z. Bai<sup>1</sup>, R. B. F. Baldini Ferroli<sup>17</sup>, Y. Ban<sup>25</sup>, J. Becker<sup>2</sup>, N. Berger<sup>1</sup>,  
 M. B. Bertani<sup>17</sup>, J. M. Bian<sup>37</sup>, E. Boger<sup>18a</sup>, O. Bondarenko<sup>19</sup>, I. Boyko<sup>18</sup>,  
 R. A. Briere<sup>3</sup>, V. Bytev<sup>18</sup>, X. Cai<sup>1</sup>, A. C. Calcaterra<sup>17</sup>, G. F. Cao<sup>1</sup>, J. F. Chang<sup>1</sup>,  
 G. Chelkov<sup>18a</sup>, G. Chen<sup>1</sup>, H. S. Chen<sup>1</sup>, J. C. Chen<sup>1</sup>, M. L. Chen<sup>1</sup>, S. J. Chen<sup>23</sup>,  
 Y. Chen<sup>1</sup>, Y. B. Chen<sup>1</sup>, H. P. Cheng<sup>13</sup>, Y. P. Chu<sup>1</sup>, D. Cronin-Hennessy<sup>37</sup>,  
 H. L. Dai<sup>1</sup>, J. P. Dai<sup>1</sup>, D. Dedovich<sup>18</sup>, Z. Y. Deng<sup>1</sup>, I. Denysenko<sup>18b</sup>,  
 M. Destefanis<sup>41</sup>, W. L. Ding<sup>27</sup>, Y. Ding<sup>21</sup>, L. Y. Dong<sup>1</sup>, M. Y. Dong<sup>1</sup>,  
 S. X. Du<sup>44</sup>, J. Fang<sup>1</sup>, S. S. Fang<sup>1</sup>, C. Q. Feng<sup>39</sup>, C. D. Fu<sup>1</sup>, J. L. Fu<sup>23</sup>, Y. Gao<sup>34</sup>,  
 C. Geng<sup>39</sup>, K. Goetzen<sup>7</sup>, W. X. Gong<sup>1</sup>, M. Greco<sup>41</sup>, M. H. Gu<sup>1</sup>, Y. T. Gu<sup>9</sup>,  
 Y. H. Guan<sup>6</sup>, A. Q. Guo<sup>24</sup>, L. B. Guo<sup>22</sup>, Y.P. Guo<sup>24</sup>, Y. L. Han<sup>1</sup>, X. Q. Hao<sup>1</sup>,  
 F. A. Harris<sup>36</sup>, K. L. He<sup>1</sup>, M. He<sup>1</sup>, Z. Y. He<sup>24</sup>, Y. K. Heng<sup>1</sup>, Z. L. Hou<sup>1</sup>,  
 H. M. Hu<sup>1</sup>, J. F. Hu<sup>6</sup>, T. Hu<sup>1</sup>, B. Huang<sup>1</sup>, G. M. Huang<sup>14</sup>, J. S. Huang<sup>11</sup>,  
 X. T. Huang<sup>27</sup>, Y. P. Huang<sup>1</sup>, T. Hussain<sup>40</sup>, C. S. Ji<sup>39</sup>, Q. Ji<sup>1</sup>, X. B. Ji<sup>1</sup>, X. L. Ji<sup>1</sup>,  
 L. K. Jia<sup>1</sup>, L. L. Jiang<sup>1</sup>, X. S. Jiang<sup>1</sup>, J. B. Jiao<sup>27</sup>, Z. Jiao<sup>13</sup>, D. P. Jin<sup>1</sup>, S. Jin<sup>1</sup>,  
 F. F. Jing<sup>34</sup>, N. Kalantar-Nayestanaki<sup>19</sup>, M. Kavatsyuk<sup>19</sup>, W. Kuehn<sup>35</sup>, W. Lai<sup>1</sup>,  
 J. S. Lange<sup>35</sup>, J. K. C. Leung<sup>33</sup>, C. H. Li<sup>1</sup>, Cheng Li<sup>39</sup>, Cui Li<sup>39</sup>, D. M. Li<sup>44</sup>,  
 F. Li<sup>1</sup>, G. Li<sup>1</sup>, H. B. Li<sup>1</sup>, J. C. Li<sup>1</sup>, K. Li<sup>10</sup>, Lei Li<sup>1</sup>, N. B. Li<sup>22</sup>, Q. J. Li<sup>1</sup>,  
 S. L. Li<sup>1</sup>, W. D. Li<sup>1</sup>, W. G. Li<sup>1</sup>, X. L. Li<sup>27</sup>, X. N. Li<sup>1</sup>, X. Q. Li<sup>24</sup>, X. R. Li<sup>26</sup>,  
 Z. B. Li<sup>31</sup>, H. Liang<sup>39</sup>, Y. F. Liang<sup>29</sup>, Y. T. Liang<sup>35</sup>, G. R. Liao<sup>34</sup>, X. T. Liao<sup>1</sup>,  
 B. J. Liu<sup>1</sup>, B. J. Liu<sup>32</sup>, C. L. Liu<sup>3</sup>, C. X. Liu<sup>1</sup>, C. Y. Liu<sup>1</sup>, F. H. Liu<sup>28</sup>, Fang Liu<sup>1</sup>,  
 Feng Liu<sup>14</sup>, H. Liu<sup>1</sup>, H. B. Liu<sup>6</sup>, H. H. Liu<sup>12</sup>, H. M. Liu<sup>1</sup>, H. W. Liu<sup>1</sup>, J. P. Liu<sup>42</sup>,  
 K. Liu<sup>6</sup>, K. Liu<sup>25</sup>, K. Y. Liu<sup>21</sup>, Q. Liu<sup>36</sup>, S. B. Liu<sup>39</sup>, X. Liu<sup>20</sup>, X. H. Liu<sup>1</sup>,  
 Y. B. Liu<sup>24</sup>, Yong Liu<sup>1</sup>, Z. A. Liu<sup>1</sup>, Zhiqiang Liu<sup>1</sup>, Zhiqing Liu<sup>1</sup>, H. Loehner<sup>19</sup>,  
 G. R. Lu<sup>11</sup>, H. J. Lu<sup>13</sup>, J. G. Lu<sup>1</sup>, Q. W. Lu<sup>28</sup>, X. R. Lu<sup>6</sup>, Y. P. Lu<sup>1</sup>, C. L. Luo<sup>22</sup>,  
 M. X. Luo<sup>43</sup>, T. Luo<sup>36</sup>, X. L. Luo<sup>1</sup>, M. Lv<sup>1</sup>, C. L. Ma<sup>6</sup>, F. C. Ma<sup>21</sup>, H. L. Ma<sup>1</sup>,  
 Q. M. Ma<sup>1</sup>, S. Ma<sup>1</sup>, T. Ma<sup>1</sup>, X. Y. Ma<sup>1</sup>, M. Maggiora<sup>41</sup>, Q. A. Malik<sup>40</sup>, H. Mao<sup>1</sup>,  
 Y. J. Mao<sup>25</sup>, Z. P. Mao<sup>1</sup>, J. G. Messchendorp<sup>19</sup>, J. Min<sup>1</sup>, T. J. Min<sup>1</sup>,  
 R. E. Mitchell<sup>16</sup>, X. H. Mo<sup>1</sup>, N. Yu. Muchnoi<sup>5</sup>, Y. Nefedov<sup>18</sup>, I. B. Nikolaev<sup>5</sup>,  
 Z. Ning<sup>1</sup>, S. L. Olsen<sup>26</sup>, Q. Ouyang<sup>1</sup>, S. P. Pacetti<sup>17c</sup>, J. W. Park<sup>26</sup>,  
 M. Pelizaesus<sup>36</sup>, K. Peters<sup>7</sup>, J. L. Ping<sup>22</sup>, R. G. Ping<sup>1</sup>, R. Poling<sup>37</sup>, C. S. J. Pun<sup>33</sup>,  
 M. Qi<sup>23</sup>, S. Qian<sup>1</sup>, C. F. Qiao<sup>6</sup>, X. S. Qin<sup>1</sup>, Z. H. Qin<sup>1</sup>, J. F. Qiu<sup>1</sup>,  
 K. H. Rashid<sup>40</sup>, G. Rong<sup>1</sup>, X. D. Ruan<sup>9</sup>, A. Sarantsev<sup>18d</sup>, J. Schulze<sup>2</sup>, M. Shao<sup>39</sup>,  
 C. P. Shen<sup>36e</sup>, X. Y. Shen<sup>1</sup>, H. Y. Sheng<sup>1</sup>, M. R. Shepherd<sup>16</sup>, X. Y. Song<sup>1</sup>,  
 S. Spataro<sup>41</sup>, B. Spruck<sup>35</sup>, D. H. Sun<sup>1</sup>, G. X. Sun<sup>1</sup>, J. F. Sun<sup>11</sup>, S. S. Sun<sup>1</sup>,  
 X. D. Sun<sup>1</sup>, Y. J. Sun<sup>39</sup>, Y. Z. Sun<sup>1</sup>, Z. J. Sun<sup>1</sup>, Z. T. Sun<sup>39</sup>, C. J. Tang<sup>29</sup>,  
 X. Tang<sup>1</sup>, E. H. Thorndike<sup>38</sup>, H. L. Tian<sup>1</sup>, D. Toth<sup>37</sup>, M. U. Ulrich<sup>35</sup>,  
 G. S. Varner<sup>36</sup>, B. Wang<sup>9</sup>, B. Q. Wang<sup>25</sup>, K. Wang<sup>1</sup>, L. L. Wang<sup>4</sup>, L. S. Wang<sup>1</sup>,  
 M. Wang<sup>27</sup>, P. Wang<sup>1</sup>, P. L. Wang<sup>1</sup>, Q. Wang<sup>1</sup>, Q. J. Wang<sup>1</sup>, S. G. Wang<sup>25</sup>,  
 X. F. Wang<sup>11</sup>, X. L. Wang<sup>39</sup>, Y. D. Wang<sup>39</sup>, Y. F. Wang<sup>1</sup>, Y. Q. Wang<sup>27</sup>,  
 Z. Wang<sup>1</sup>, Z. G. Wang<sup>1</sup>, Z. Y. Wang<sup>1</sup>, D. H. Wei<sup>8</sup>, Q. G. Wen<sup>39</sup>, S. P. Wen<sup>1</sup>,

M. W. Werner<sup>35</sup>, U. Wiedner<sup>2</sup>, L. H. Wu<sup>1</sup>, N. Wu<sup>1</sup>, W. Wu<sup>24</sup>, Z. Wu<sup>1</sup>,  
L. G. Xia<sup>34</sup>, Z. J. Xiao<sup>22</sup>, Y. G. Xie<sup>1</sup>, Q. L. Xiu<sup>1</sup>, G. F. Xu<sup>1</sup>, G. M. Xu<sup>25</sup>, H. Xu<sup>1</sup>,  
Q. J. Xu<sup>10</sup>, X. P. Xu<sup>30</sup>, Y. Xu<sup>24</sup>, Z. R. Xu<sup>39</sup>, F. Xue<sup>14</sup>, Z. Xue<sup>1</sup>, L. Yan<sup>39</sup>,  
W. B. Yan<sup>39</sup>, Y. H. Yan<sup>15</sup>, H. X. Yang<sup>1</sup>, T. Yang<sup>9</sup>, Y. Yang<sup>14</sup>, Y. X. Yang<sup>8</sup>,  
H. Ye<sup>1</sup>, M. Ye<sup>1</sup>, M. H. Ye<sup>4</sup>, B. X. Yu<sup>1</sup>, C. X. Yu<sup>24</sup>, S. P. Yu<sup>27</sup>, C. Z. Yuan<sup>1</sup>, W. L.  
Yuan<sup>22</sup>, Y. Yuan<sup>1</sup>, A. A. Zafar<sup>40</sup>, A. Z. Zallo<sup>17</sup>, Y. Zeng<sup>15</sup>, B. X. Zhang<sup>1</sup>,  
B. Y. Zhang<sup>1</sup>, C. C. Zhang<sup>1</sup>, D. H. Zhang<sup>1</sup>, H. H. Zhang<sup>31</sup>, H. Y. Zhang<sup>1</sup>,  
J. Zhang<sup>22</sup>, J. Q. Zhang<sup>1</sup>, J. W. Zhang<sup>1</sup>, J. Y. Zhang<sup>1</sup>, J. Z. Zhang<sup>1</sup>, L. Zhang<sup>23</sup>,  
S. H. Zhang<sup>1</sup>, T. R. Zhang<sup>22</sup>, X. J. Zhang<sup>1</sup>, X. Y. Zhang<sup>27</sup>, Y. Zhang<sup>1</sup>,  
Y. H. Zhang<sup>1</sup>, Y. S. Zhang<sup>9</sup>, Z. P. Zhang<sup>39</sup>, Z. Y. Zhang<sup>42</sup>, G. Zhao<sup>1</sup>, H. S. Zhao<sup>1</sup>,  
Jingwei Zhao<sup>1</sup>, Lei Zhao<sup>39</sup>, Ling Zhao<sup>1</sup>, M. G. Zhao<sup>24</sup>, Q. Zhao<sup>1</sup>, S. J. Zhao<sup>44</sup>,  
T. C. Zhao<sup>1</sup>, X. H. Zhao<sup>23</sup>, Y. B. Zhao<sup>1</sup>, Z. G. Zhao<sup>39</sup>, A. Zhemchugov<sup>18a</sup>,  
B. Zheng<sup>1</sup>, J. P. Zheng<sup>1</sup>, Y. H. Zheng<sup>6</sup>, Z. P. Zheng<sup>1</sup>, B. Zhong<sup>1</sup>, J. Zhong<sup>2</sup>,  
L. Zhou<sup>1</sup>, X. K. Zhou<sup>6</sup>, X. R. Zhou<sup>39</sup>, C. Zhu<sup>1</sup>, K. Zhu<sup>1</sup>, K. J. Zhu<sup>1</sup>, S. H. Zhu<sup>1</sup>,  
X. L. Zhu<sup>34</sup>, X. W. Zhu<sup>1</sup>, Y. S. Zhu<sup>1</sup>, Z. A. Zhu<sup>1</sup>, J. Zhuang<sup>1</sup>, B. S. Zou<sup>1</sup>,  
J. H. Zou<sup>1</sup>, J. X. Zuo<sup>1</sup>

(BESIII Collaboration)

- <sup>1</sup> *Institute of High Energy Physics, Beijing 100049, P. R. China*  
<sup>2</sup> *Bochum Ruhr-University, 44780 Bochum, Germany*  
<sup>3</sup> *Carnegie Mellon University, Pittsburgh, PA 15213, USA*  
<sup>4</sup> *China Center of Advanced Science and Technology,  
Beijing 100190, P. R. China*  
<sup>5</sup> *G.I. Budker Institute of Nuclear Physics SB RAS (BINP),  
Novosibirsk 630090, Russia*  
<sup>6</sup> *Graduate University of Chinese Academy of Sciences,  
Beijing 100049, P. R. China*  
<sup>7</sup> *GSI Helmholtzcentre for Heavy Ion Research GmbH,  
D-64291 Darmstadt, Germany*  
<sup>8</sup> *Guangxi Normal University, Guilin 541004, P. R. China*  
<sup>9</sup> *GuangXi University, Nanning 530004, P.R.China*  
<sup>10</sup> *Hangzhou Normal University, XueLin Jie 16,  
Xiasha Higher Education Zone Hangzhou, 310036, P. R. China*  
<sup>11</sup> *Henan Normal University, Xinxiang 453007, P. R. China*  
<sup>12</sup> *Henan University of Science and Technology,  
13 Huangshan College, Huangshan 245000, P. R. China*  
<sup>14</sup> *Huazhong Normal University, Wuhan 430079, P. R. China*  
<sup>15</sup> *Hunan University, Changsha 410082, P. R. China*  
<sup>16</sup> *Indiana University, Bloomington, Indiana 47405, USA*  
<sup>17</sup> *INFN Laboratori Nazionali di Frascati, Frascati, Italy*  
<sup>18</sup> *Joint Institute for Nuclear Research, 141980 Dubna, Russia*  
<sup>19</sup> *KVI/University of Groningen, 9747 AA Groningen, The Netherlands*  
<sup>20</sup> *Lanzhou University, Lanzhou 730000, P. R. China*  
<sup>21</sup> *Liaoning University, Shenyang 110036, P. R. China*  
<sup>22</sup> *Nanjing Normal University, Nanjing 210046, P. R. China*

- <sup>23</sup> *Nanjing University, Nanjing 210093, P. R. China*
- <sup>24</sup> *Nankai University, Tianjin 300071, P. R. China*
- <sup>25</sup> *Peking University, Beijing 100871, P. R. China*
- <sup>26</sup> *Seoul National University, Seoul, 151-747 Korea*
- <sup>27</sup> *Shandong University, Jinan 250100, P. R. China*
- <sup>28</sup> *Shanxi University, Taiyuan 030006, P. R. China*
- <sup>29</sup> *Sichuan University, Chengdu 610064, P. R. China*
- <sup>30</sup> *Soochow University, Suzhou 215006, China*
- <sup>31</sup> *Sun Yat-Sen University, Guangzhou 510275, P. R. China*
- <sup>32</sup> *The Chinese University of Hong Kong, Shatin, N.T., Hong Kong.*
- <sup>33</sup> *The University of Hong Kong, Pokfulam, Hong Kong*
- <sup>34</sup> *Tsinghua University, Beijing 100084, P. R. China*
- <sup>35</sup> *Universitaet Giessen, 35392 Giessen, Germany*
- <sup>36</sup> *University of Hawaii, Honolulu, Hawaii 96822, USA*
- <sup>37</sup> *University of Minnesota, Minneapolis, MN 55455, USA*
- <sup>38</sup> *University of Rochester, Rochester, New York 14627, USA*
- <sup>39</sup> *University of Science and Technology of China, Hefei 230026, P. R. China*
- <sup>40</sup> *University of the Punjab, Lahore-54590, Pakistan*
- <sup>41</sup> *University of Turin and INFN, Turin, Italy*
- <sup>42</sup> *Wuhan University, Wuhan 430072, P. R. China*
- <sup>43</sup> *Zhejiang University, Hangzhou 310027, P. R. China*
- <sup>44</sup> *Zhengzhou University, Zhengzhou 450001, P. R. China*
- <sup>a</sup> *also at the Moscow Institute of Physics and Technology, Moscow, Russia*
- <sup>b</sup> *on leave from the Bogolyubov Institute for Theoretical Physics, Kiev, Ukraine*
- <sup>c</sup> *Currently at University of Perugia and INFN, Perugia, Italy*
- <sup>d</sup> *also at the PNPI, Gatchina, Russia*
- <sup>e</sup> *now at Nagoya University, Nagoya, Japan*

---

**Abstract**

We study the decays of the  $J/\psi$  and  $\psi'$  mesons to  $\pi^+\pi^-\pi^0$  using data samples at both resonances collected with the BES III detector in 2009. We measure the corresponding branching fractions with unprecedented precision and provide mass spectra and Dalitz plots. The branching fraction for  $J/\psi \rightarrow \pi^+\pi^-\pi^0$  is determined to be

$$(2.137 \pm 0.004 \text{ (stat.)}_{-0.056}^{+0.058} \text{ (syst.)}_{-0.026}^{+0.027} \text{ (norm.)}) \times 10^{-2},$$

and the branching fraction for  $\psi' \rightarrow \pi^+\pi^-\pi^0$  is measured as

$$(2.14 \pm 0.03 \text{ (stat.)}_{-0.07}^{+0.08} \text{ (syst.)}_{-0.08}^{+0.09} \text{ (norm.)}) \times 10^{-4}.$$

The  $J/\psi$  decay is found to be dominated by an intermediate  $\rho(770)$  state, whereas the  $\psi'$  decay is dominated by di-pion masses around  $2.2 \text{ GeV}/c^2$ , leading to strikingly different Dalitz distributions.

*Keywords:*

BES III, Hadronic charmonium decays

---

## 1. Introduction

Previous studies of  $J/\psi \rightarrow \pi^+\pi^-\pi^0$  [1, 2, 3, 4] and  $\psi' \rightarrow \pi^+\pi^-\pi^0$  [1, 5, 6] found not only an unexpectedly low branching fraction in the case of the  $\psi'$ <sup>1</sup> (world averages:  $BF(J/\psi \rightarrow \pi^+\pi^-\pi^0) = (2.07 \pm 0.12) \times 10^{-2}$  and  $BF(\psi' \rightarrow \pi^+\pi^-\pi^0) = (1.68 \pm 0.26) \times 10^{-4}$  [8]) but also a completely different shape of the di-pion mass spectrum and the Dalitz plot. The fact that the  $\rho(770)\pi$  decays as a fraction of all hadronic decays are suppressed by two orders of magnitude in the  $\psi'$  with regards to the  $J/\psi$  is especially difficult to explain and known as the  $\rho\pi$  puzzle. Suggested solutions include intrinsic charm in the light vector mesons [7], formation of three-gluon intermediate

---

<sup>1</sup>Some authors [7] claim that the  $\psi' \rightarrow \pi^+\pi^-\pi^0$  branching fraction is as expected and the  $J/\psi \rightarrow \pi^+\pi^-\pi^0$  fraction is much higher than expected for a  $c\bar{c}$  model of the  $J/\psi$ .

resonances [9], a hybrid nature of the  $\psi'$  [10], an additional hadronic amplitude for the  $\psi'$  decays [11], the  $J/\psi$  being dominantly a higher Fock-state [12] and so on.

In this letter we present new measurements of the  $J/\psi \rightarrow \pi^+\pi^-\pi^0$  and  $\psi' \rightarrow \pi^+\pi^-\pi^0$  branching fractions with unprecedented precision using the large data samples collected with the BES III detector at the  $J/\psi$  and  $\psi'$  resonances. These measurements are an important first step to an experimental inquiry into the puzzle of the decay dynamics, preparing the way for a detailed analysis. The large branching fraction of  $J/\psi \rightarrow \pi^+\pi^-\pi^0$  also makes it an important background process for many other studies (e.g. the scalar meson spectrum in  $J/\psi \rightarrow \gamma\pi^+\pi^-$ ), an improved knowledge of this branching fraction will thus also enhance the precision of those measurements.

## 2. Detector and Monte Carlo Simulation

BEPC II is a double-ring  $e^+e^-$  collider designed to provide a peak luminosity of  $10^{33} \text{ cm}^{-2}\text{s}^{-1}$  at a beam current of 0.93 A. The BES III [13] detector has a geometrical acceptance of 93% of  $4\pi$  and has four main components: (1) A small-cell, helium-based (40% He, 60%  $\text{C}_3\text{H}_8$ ) main drift chamber (MDC) with 43 layers providing an average single-hit resolution of  $135 \mu\text{m}$ , charged-particle momentum resolution in a 1 T magnetic field of 0.5% at  $1 \text{ GeV}/c$ , and a  $dE/dx$  resolution that is better than 6%. (2) An electromagnetic calorimeter (EMC) consisting of 6240 CsI(Tl) crystals in a cylindrical structure (barrel) and two end caps. The energy resolution at  $1.0 \text{ GeV}/c$  is 2.5% (5%) in the barrel (end caps), and the position resolution is 6 mm (9 mm) in the barrel (end caps). (3) A time-of-flight system (TOF) constructed of 5-cm-thick plastic scintillators, with 176 detectors of 2.4 m length in two layers in the barrel and 96 fan-shaped detectors in the end caps. The barrel (end cap) time resolution of 80 ps (110 ps) provides a  $2\sigma$   $K/\pi$  separation for momenta up to  $\sim 1.0 \text{ GeV}/c$ . (4) The muon system (MUC) consists of  $1000 \text{ m}^2$  of Resistive Plate Chambers (RPCs) in nine barrel and eight end cap layers and provides 2 cm position resolution.

For the events to be read-out, one out of seven trigger conditions based on combinations of signals from the MDC, TOF and EMC had to be fulfilled. At least one of these rather loose conditions should always be fulfilled for the events under study, and indeed overall trigger efficiencies very close to 100% were found for hadronic events containing charged particles [14].

The efficiencies of the detector and the event selection are estimated using a Monte Carlo (MC) simulation based on GEANT4 [15, 16]. EVTGEN [17]

is used to generate events; for the  $J/\psi \rightarrow \pi^+\pi^-\pi^0$  decay,  $\rho(770)\pi$  events give a good description of the data, while for  $\psi' \rightarrow \pi^+\pi^-\pi^0$  a mixture of  $\rho(770)\pi$  and  $P$ -wave phase-space events is used<sup>2</sup>. In both cases, differences between the generated and observed distributions are taken care of by reweighting the MC events to the data distribution in the Dalitz variables. For the estimation of backgrounds, inclusive MC samples are generated by KKMC [18, 19] — known decays of the  $J/\psi$  and  $\psi'$  are modeled by EVTGEN according to the branching fractions provided by the Particle Data Group (PDG) [8], and the remaining unknown decay modes are generated with LUNDCHARM [17]. Backgrounds from the process  $J/\psi \rightarrow \gamma\pi^+\pi^-$  have been modeled using amplitudes extracted from a partial wave analysis of BES III data.

### 3. Data Samples and Event Selection

This analysis uses a sample of  $2.25 \times 10^8$   $J/\psi$  decays [20] and  $1.06 \times 10^8$   $\psi'$  decays [21] collected by BES III in 2009.

Charged particle tracks in BES III are reconstructed using MDC hits. We require tracks to pass within  $\pm 10$  cm from the interaction point in the beam direction, within 1 cm of the beam line in the plane perpendicular to the beam and to have a polar angle in the range  $|\cos\vartheta| < 0.93$ . Events are required to contain exactly one track of positive and one of negative charge, corresponding to the  $\pi^+$  and  $\pi^-$ . Electromagnetic showers are reconstructed by clustering EMC crystal energies [22]. The energy deposit in nearby TOF counters is included in order to improve the reconstruction efficiency and energy resolution. Showers identified as photon candidates must satisfy fiducial, timing and shower-quality requirements. Showers from the barrel region ( $|\cos\vartheta| < 0.8$ ) are required to have an energy above 25 MeV, while those in the end caps ( $0.86 < |\cos\vartheta| < 0.92$ ) must have at least 50 MeV. Showers from the transition region between barrel and end cap are excluded from the analysis, as are showers within  $10^\circ$  from any charged track. Events are required to contain at least two showers fulfilling these criteria.

For every pair of photon candidates, a full event kinematic fit with the

---

<sup>2</sup>The use of  $P$ -wave phase space (and subsequent reweighting in the Dalitz-variables) is motivated by the angular distributions and the fact that not much is known about the dynamics leading to the accumulation of events around a di-pion mass of  $2.2 \text{ GeV}/c^2$ . This procedure has been checked using both toy MC samples and a sample generated using the amplitudes extracted from a phenomenological fit to the data. The maximum difference in efficiency obtained is taken as a systematic error.

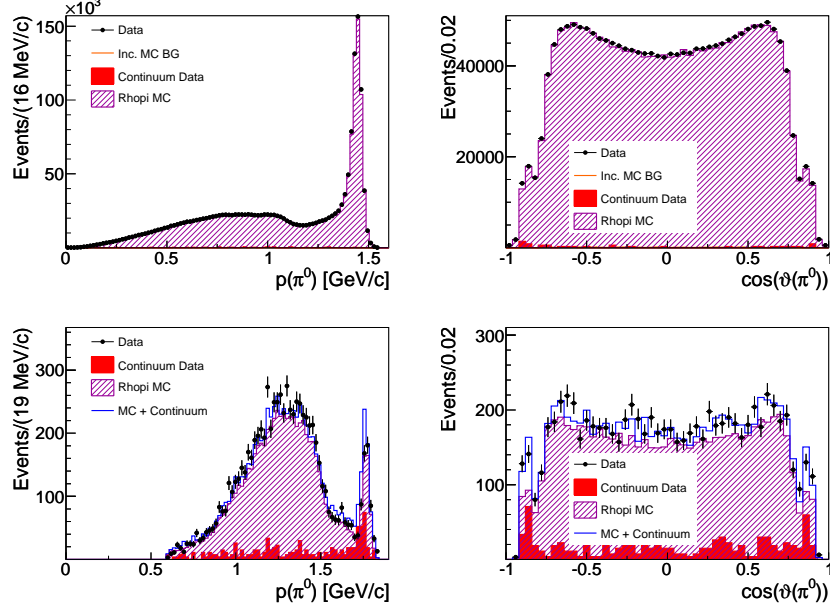


Figure 1: Kinematical distributions of the reconstructed  $\pi^0$ s: Top for the  $J/\psi \rightarrow \pi^+\pi^-\pi^0$  analysis, bottom for the  $\psi' \rightarrow \pi^+\pi^-\pi^0$  analysis; left showing the  $\pi^0$  momentum, right showing the  $\pi^0$  polar angle distributions.

initial particle ( $J/\psi$  or  $\psi'$ ) four-momentum as a constraint is performed. The pair leading to the smallest  $\chi^2$  is kept as the  $\pi^0$  candidate if  $\chi^2 < 50$ , otherwise, the event is rejected. The fit is repeated once more with the assumption that the charged particles are kaons; if this leads to a smaller  $\chi^2$ , the event is also rejected. Yet another kinematic fit is performed with the mass of the  $\pi^0$  as an additional constraint; the resulting  $\chi^2$  is required to be less than 50. The invariant mass of the two photon candidates has to be compatible with the mass of the  $\pi^0$ ,  $0.11 \text{ GeV}/c^2 < m_{\gamma\gamma} < 0.15 \text{ GeV}/c^2$ .

For the  $\psi' \rightarrow \pi^+\pi^-\pi^0$  analysis, additional requirements are needed to suppress backgrounds from radiative decays to  $e^+e^-$ ,  $\mu^+\mu^-$  and the  $J/\psi$  and  $\chi_c$  states, namely the invariant mass of the charged pion candidates is required to be less than  $3 \text{ GeV}/c^2$ , the energy deposits associated to the tracks is required to be less than  $0.8 \text{ GeV}$  and the penetration depth into the muon system less than  $40 \text{ cm}$ .

#### 4. Efficiency correction

In order to study differences between the simulation and data in track reconstruction, an analysis of a specially selected  $J/\psi$  to  $3\pi$  candidate subsample with one or two tracks and two or more photons and with tight requirements on one track and the  $\pi^0$  is performed. Specifically, the TOF and  $\frac{dE}{dx}$  information of the charged track are combined to form particle identification confidence levels for the  $\pi$  and  $K$  hypotheses; the likelihood for the  $\pi$  hypothesis is then required to be larger than the likelihood for the  $K$  hypothesis. Kinematic fits to the  $\pi^0$  mass are performed for all pairs of photon candidates, and the pair with the lowest  $\chi^2$  is taken as the  $\pi^0$  candidate, if the  $\chi^2$  is less than 20. The invariant mass of the object recoiling against the system of the track and the  $\pi^0$  is required to be between 0 and 0.2 GeV/ $c^2$ , and the recoil direction must be within the tracker acceptance. Using these tagged events, the efficiency for finding and correctly reconstructing the second track is determined. The simulation is then corrected as a function of polar angle and track momentum to reflect the efficiency found in data (which is on average about 2% lower than the simulated efficiency).

Similarly, an analysis using a subsample similar to the one above but requiring two tracks and with tight requirements on the two tracks and photons, chosen with the standard photon selection, is performed to test the  $\pi^0$  reconstruction efficiency. The tracks are again required to pass particle identification requirements as above and in addition are required to have an associated energy deposit in the calorimeter of less than 0.8 times the beam energy to remove electrons and a penetration depth in the muon system less than 40 cm to remove muons. Their opening angle is required to be less than  $170^\circ$ . The momentum of the system recoiling against the tracks must be larger than 100 MeV/ $c$ , and the invariant mass of the tracks and the two photon candidates must be above 3.0 GeV/ $c^2$ . Here the efficiency differences found between selected data and simulated events (of the order of 0.5%) are used to correct the simulation as a function of  $\pi^0$  momentum. Figure 1 shows the reconstructed kinematics of the  $\pi^0$  for the selected events compared to the corrected MC simulation.

#### 5. Results

1,859,771 events from the  $J/\psi$  sample and 7872 events from the  $\psi'$  sample survive all selection criteria. The branching fractions are calculated as follows:

$$BF = \frac{N_{sel} - N_{continuum}^{BG} - N_{resonance}^{BG}}{N_\psi \cdot \epsilon_{MC} \cdot \epsilon_{trig} \cdot BF(\pi^0 \rightarrow \gamma\gamma)}, \quad (1)$$



Quantity	$J/\psi \longrightarrow \pi^+\pi^-\pi^0$	$\psi' \longrightarrow \pi^+\pi^-\pi^0$
$N_{sel}$	$1859771 \pm 1364$	$7872 \pm 89$
$N_{continuum}^{BG}$	$8811 \pm 1582$	$820 \pm 55$
$N_{resonance}^{BG}$	$9919 \pm 463$	$101 \pm 32$
$N_\psi$	$(225.2 \pm 2.8)$ Million	$(106.4 \pm 4)$ Million
$\epsilon_{MC}$	$38.66 \pm 0.05$	$30.91 \pm 0.14$
$\epsilon_{trig}$	$(100 - 0.2)\%$ [14]	
$BF(\pi^0 \rightarrow \gamma\gamma)$	$(98.823 \pm 0.023)\%$ [8]	

Table 1: Numbers used in the branching fraction calculation

where  $N_{sel}$  is the number of selected events,  $N_{continuum}^{BG}$  the number of background events from the continuum (estimated from data samples taken at 3.08 GeV and 3.65 GeV),  $N_{resonance}^{BG}$  the number of background events from other resonance processes (estimated using inclusive MC samples) and  $N_\psi$  the number of  $J/\psi$  or  $\psi'$  mesons in the sample.  $\epsilon_{MC}$  is the efficiency determined from signal MC,  $\epsilon_{trig}$  is the trigger efficiency (found to be very close to 100%, [14]), and the branching fraction for  $\pi^0 \rightarrow \gamma\gamma$  is taken from the PDG [8] — the corresponding numbers can be found in table 1. In this calculation, interference of resonance and continuum processes is neglected.

Possible systematic errors resulting from the following sources were studied:

- The uncertainty due to the simulation model was estimated by the difference in the efficiency with and without the reweighting described in section 2 for the  $J/\psi$  sample and by comparing with the efficiency obtained from a sample generated using amplitudes extracted from a phenomenological fit<sup>3</sup> for the  $\psi'$  sample. For both cases, the model error is not the dominant systematic error.
- The absolute energy scale of the EMC is known to an accuracy of 0.4% [23];
- The photon detection and reconstruction efficiency is described by the simulation to within 1% per photon [23].

<sup>3</sup>In this fit, contributions from  $\rho(770)$ , a higher  $\rho$  with a mass of 2285 MeV/ $c^2$  and a width of 950 MeV/ $c^2$  and a  $\rho^3$  with a mass of 1750 MeV/ $c^2$  and a width of 650 MeV/ $c^2$  were found to lead to an adequate description of the data.

Source of systematic	$J/\psi \longrightarrow \pi^+\pi^-\pi^0$		$\psi' \longrightarrow \pi^+\pi^-\pi^0$	
	Upward Change (%)	Downward Change (%)	Upward Change (%)	Downward Change (%)
MC simulation	0.25	-0.23	1.20	-1.20
EMC Energy scale	0.02	-0.02	0.18	-0.15
$\gamma$ efficiency	2.04	-1.96	2.04	-1.96
$\pi^0$ kinematic fit	0.28	-0.27	0.27	-0.27
tracking efficiency	1.64	-1.59	1.80	-1.75
Muon cut	—	—	1.28	-0.75
Trigger efficiency	0.20	0.00	0.20	0.00
Resonance background	0.67	-0.67	1.45	-1.45
Syst. w/o normalization	2.74	-2.64	3.57	3.33
Normalization	1.26	-1.23	4.17	-3.85
Total syst. uncertainty	3.01	-2.91	5.49	5.09
Syst. + stat. uncertainty	3.02	-2.91	5.72	5.34

Table 2: Impact of the systematic uncertainties on the measured branching fractions; the various sources of systematic uncertainties lead to the listed upward and downward changes in the branching fractions.

- The uncertainty due to the  $\pi^0$  finding and kinematic fitting was estimated by performing a different analysis with the  $J/\psi$  data sample (see section 4). A tighter selection was applied to the charged tracks and no  $\pi^0$  was required. The difference between data and simulation is taken as the systematic error.
- The uncertainty due to charged particle track finding and kinematic fitting was estimated using an analysis with tight requirements on the  $\pi^0$  and one charged track. The efficiencies for finding and reconstructing the other track were compared between data and simulation (see section 4).
- The efficiency of the muon rejection (used only in the  $\psi'$  analysis) was estimated by either dropping the requirement or demanding a penetration less than 30 cm instead of less than 40 cm.
- The trigger efficiency was changed from 100% to 99.8%, reflecting the statistical uncertainty of the efficiency determination [14].
- The background from continuum processes was estimated using samples taken off-resonance ( $282 \text{ nb}^{-1}$  of luminosity taken at a center-of-

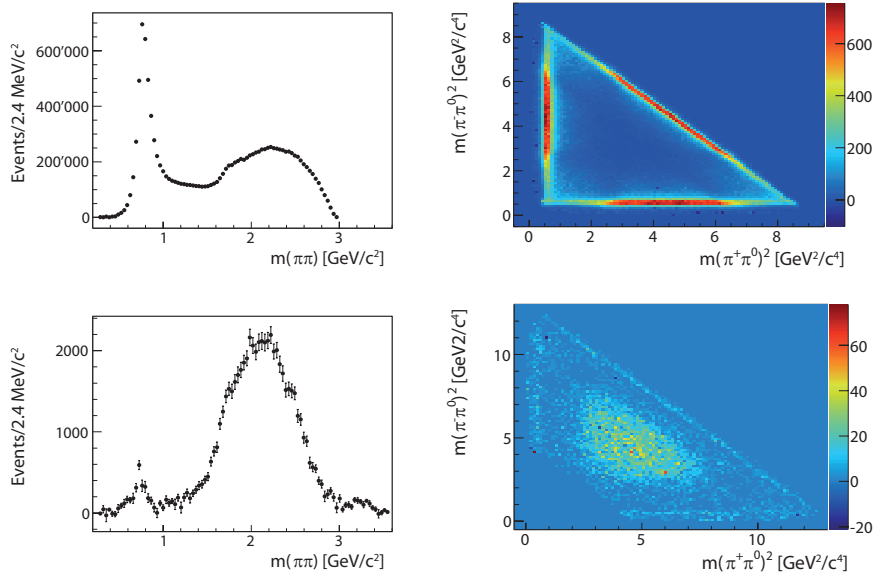


Figure 2:  $\pi\pi$  invariant mass distribution (left) and Dalitz plot (right) with backgrounds subtracted and corrected for efficiency. Top and bottom graphs show the results for the  $J/\psi \rightarrow \pi^+\pi^-\pi^0$  and  $\psi' \rightarrow \pi^+\pi^-\pi^0$  analysis, respectively.

mass energy of 3.08 GeV, compared to 81 pb<sup>-1</sup> at the  $J/\psi$  resonance and 43 pb<sup>-1</sup> taken at a center-of-mass energy of 3.650 GeV, compared to 163 pb<sup>-1</sup> at the  $\psi'$  resonance). The small samples due to the clean selection lead to relatively large statistical errors for the continuum contribution (18.0% for the  $J/\psi$  and 6.7% for the  $\psi'$ ). Compared to these errors the systematic errors from the luminosity measurements or varying beam conditions can be neglected.

- The accuracy of the inclusive simulation for describing background from resonant processes was checked in analyses requiring one photon less (a  $\pi^+\pi^-\gamma$  final state) or one photon more (a  $\pi^+\pi^-\pi^0\gamma$  final state) and was found to be mediocre; it is assigned an uncertainty of 100%.
- The normalization (number of  $J/\psi$  or  $\psi'$  events) has an uncertainty of 1.23% for the  $J/\psi$  sample [20] and 4% for the  $\psi'$  sample [21].

Table 2 shows the impact of the systematic errors on the measured branching fractions.

The branching fraction for  $J/\psi \rightarrow \pi^+\pi^-\pi^0$  is determined to be

$$(2.137 \pm 0.004 \text{ (stat.)}_{-0.056}^{+0.058} \text{ (syst.)}_{-0.026}^{+0.027} \text{ (norm.)}) \times 10^{-2},$$

and the branching fraction for  $\psi' \rightarrow \pi^+\pi^-\pi^0$  is measured as

$$(2.14 \pm 0.03 \text{ (stat.)}_{-0.07}^{+0.08} \text{ (syst.)}_{-0.08}^{+0.09} \text{ (norm.)}) \times 10^{-4}.$$

Invariant mass spectra and Dalitz plots are shown in figure 2. The decay  $J/\psi \rightarrow \pi^+\pi^-\pi^0$  is dominated by  $\rho(770)$  production; the absence of events in the center of the Dalitz plot points to negatively interfering higher  $\rho$  states. In the case of the  $\psi' \rightarrow \pi^+\pi^-\pi^0$  decay, a small  $\rho(770)$  contribution can be discerned. Most of the events are however clustering around 2.2 GeV/ $c^2$  in di-pion mass. To disentangle the contributions of various excited  $\rho$  states to this peak will require a partial wave analysis.

## 6. Conclusion

The branching fractions for  $J/\psi \rightarrow \pi^+\pi^-\pi^0$  and  $\psi' \rightarrow \pi^+\pi^-\pi^0$  have been measured with unprecedented precision at the BES III experiment. The measurement for  $J/\psi \rightarrow \pi^+\pi^-\pi^0$  is in good agreement with the world average of  $BF(J/\psi \rightarrow \pi^+\pi^-\pi^0) = (2.07 \pm 0.12) \times 10^{-2}$  [8] while the result for  $\psi' \rightarrow \pi^+\pi^-\pi^0$  is slightly larger than the world average of  $BF(\psi' \rightarrow \pi^+\pi^-\pi^0) = (1.68 \pm 0.26) \times 10^{-4}$  [8]. The ratio of these two branching fractions

$$\frac{BF(\psi' \rightarrow \pi^+\pi^-\pi^0)}{BF(J/\psi \rightarrow \pi^+\pi^-\pi^0)} = (1.00 \pm 0.01 \text{ (stat.)}_{-0.05}^{+0.06} \text{ (syst.)})\%,$$

where correlations between the systematic errors of the two analyses have been taken into account, is found to be an order of magnitude smaller than the ratio of 12% naively expected from the fraction of decays via three gluon exchange.

The decay dynamics of the  $J/\psi$  are dominated by the  $\rho(770)$  meson. While the  $\rho(770)$  is also visible in the case of the  $\psi'$  decay, the dynamics there is dominated by states at higher masses. Understanding the nature of these higher mass states and why they are suppressed in  $J/\psi$  decays and enhanced in  $\psi'$  decays may be clarified in a partial wave analysis, which is beyond the scope of this letter.

## 7. Acknowledgement

The BESIII collaboration thanks the staff of BEPCII and the computing center for their hard efforts. This work is supported in part by the Ministry of Science and Technology of China under Contract No. 2009CB825200; National Natural Science Foundation of China (NSFC) under Contracts Nos. 10625524, 10821063, 10825524, 10835001, 10935007; Joint Funds of the National Natural Science Foundation of China under Contract No. 11079008; the Chinese Academy of Sciences (CAS) Large-Scale Scientific Facility Program; CAS under Contracts Nos. KJCX2-YW-N29, KJCX2-YW-N45; 100 Talents Program of CAS; Istituto Nazionale di Fisica Nucleare, Italy; Siberian Branch of Russian Academy of Science, joint project No 32 with CAS; U. S. Department of Energy under Contracts Nos. DE-FG02-04ER41291, DE-FG02-91ER40682, DE-FG02-94ER40823; U.S. National Science Foundation; University of Groningen (RuG) and the Helmholtzzentrum fuer Schwerionenforschung GmbH (GSI), Darmstadt; WCU Program of National Research Foundation of Korea under Contract No. R32-2008-000-10155-0; Swiss National Science Foundation.

## References

- [1] M. E. B. Franklin, et al., Measurement of  $\psi(3097)$  and  $\psi'$  (3686) decays into selected hadronic modes, *Phys. Rev. Lett.* 51 (1983) 963.
- [2] J. Z. Bai, et al., Measurement of the Branching Fraction of  $J/\psi \rightarrow \pi^+\pi^-\pi^0$ , *Phys. Rev. D* 70 (2004) 012005.
- [3] B. Aubert, et al., Study of  $e^+e^-$  to  $\pi^+\pi^-\pi^0$  process using initial state radiation with BaBar, *Phys. Rev. D* 70 (2004) 072004.
- [4] B. Aubert, et al., The  $e^+e^-$  to  $2(\pi^+\pi^-)\pi^0$ ,  $2(\pi^+\pi^-)\eta$ ,  $K^+K^-\pi^+\pi^-\pi^0$  and  $K^+K^-\pi^+\pi^-\eta$  Cross Sections Measured with Initial-State Radiation, *Phys. Rev. D* 76 (2007) 092005.
- [5] N. E. Adam, et al., Observation of  $1^-(0^-)$  final states from  $\psi(2S)$  decays and  $e^+e^-$  annihilation, *Phys. Rev. Lett.* 94 (2005) 012005.
- [6] M. Ablikim, et al., Partial wave analysis of  $\psi' \rightarrow \pi^+\pi^-\pi^0$  at BESII, *Phys. Lett.* B619 (2005) 247–254.
- [7] S. Brodsky, M. Karliner, Intrinsic charm of vector mesons: A possible solution of the *rho pi puzzle*, *Phys. Rev. Lett.* 78 (1997) 4682–4685.

- [8] K. Nakamura, et al., Review of particle physics, J.Phys.G G37 (2010) 075021.
- [9] S. Brodsky, G. P. Lepage, S. F. Tuan, Exclusive charmonium decays: The  $J/\psi$  ( $\psi'$ )  $\rightarrow \rho\pi, K^*\bar{K}$  puzzle, Phys. Rev. Lett. 59 (1987) 621.
- [10] L. Kisslinger, D. Parno, S. Riordan, Hybrid Charmonium and the  $\rho-\pi$  Puzzle, Adv. High Energy Phys. 2009 (2009) 982341.
- [11] M. Suzuki, Possible hadronic excess in  $\psi$  (2S) decay and the rho pi puzzle, Phys. Rev. D63 (2001) 054021.
- [12] Y. Chen, E. Braaten, An Explanation for the rho-pi Puzzle of  $J/\psi$  and  $\psi'$  Decays, Phys. Rev. Lett. 80 (1998) 5060–5063.
- [13] M. Ablikim, et al., Design and Construction of the BESIII Detector, Nucl.Instrum.Meth. A614 (2010) 345–399.
- [14] N. Berger, et al., Trigger efficiencies at BES III, Chin. Phys. C34 (2010) 1779.
- [15] S. Agostinelli, et al., GEANT4: A Simulation toolkit, Nucl.Instrum.Meth. A506 (2003) 250–303.
- [16] J. Allison, K. Amako, J. Apostolakis, H. Araujo, P. Dubois, et al., Geant4 developments and applications, IEEE Trans.Nucl.Sci. 53 (2006) 270.
- [17] R. Ping, Event generators at BES III, Chin. Phys. C 32 (2008) 599.
- [18] S. Jadach, B. Ward, Z. Was, The Precision Monte Carlo event generator KK for two fermion final states in  $e^+e^-$  collisions, Comput.Phys.Commun. 130 (2000) 260–325.
- [19] S. Jadach, B. Ward, Z. Was, Coherent exclusive exponentiation for precision Monte Carlo calculations, Phys.Rev. D63 (2001) 113009.
- [20] M. Ablikim, et al., Measurement of the Matrix Element for the Decay  $\eta' \rightarrow \eta\pi^+\pi^-$ , Phys. Rev. D83 (2011) 012003.
- [21] M. Ablikim, et al., Branching fraction measurements of  $\chi_{c0}$  and  $\chi_{c2}$  to  $\pi^0\pi^0$  and  $\eta\eta$ , Phys. Rev. D81 (2010) 052005.
- [22] M. He, Simulation and reconstruction of the BESIII EMC, Journal of Physics: Conference Series 293 (2011) 012025.

- [23] M. Ablikim, et al., Measurements of  $h_c(^1P_1)$  in  $\psi'$  Decays, Phys. Rev. Lett. 104 (2010) 132002.